Continuous Authentication Using One-Dimensional Multi-Resolution Local Binary Patterns (1DMRLBP) in ECG Biometrics

Wael Louis, *Student Member, IEEE*, Majid Komeili, *Student Member, IEEE*, and Dimitrios Hatzinakos, *Fellow, IEEE*

***Abstract*— The objective of a continuous authentication system is to continuously monitor the identity of subjects using biometric systems. In this paper, we proposed a novel feature extraction and a unique continuous authentication strategy and technique. We proposed One-Dimensional Multi-Resolution Local Binary Patterns (1DMRLBP), an online feature extraction for one-dimensional signals. We also proposed a continuous authentication system, which uses sequential sampling and 1DMRLBP feature extraction. This system adaptively updates decision thresholds and sample size during run-time. Unlike most other local binary patterns variants, 1DMRLBP accounts for observations' temporal changes and has a mechanism to extract one feature vector that represents multiple observations. 1DMRLBP also accounts for quantization error, tolerates noise, and extracts local and global signal morphology. This paper examined electrocardiogram signals. When 1DMRLBP was applied on the University of Toronto database (UofTDB) 1,012 single session subjects database, an equal error rate (EER) of 7.89% was achieved in comparison to 12.30% from a state-of-the-art work. Also, an EER of 10.10% was resulted when 1DMRLBP was applied to UofTDB 82 multiple sessions database. Experiments showed that using 1DMRLBP improved EER by 15% when compared with a biometric system based on raw time-samples. Finally, when 1DMRLBP was implemented with sequential sampling to achieve a continuous authentication system, 0.39% false rejection rate and 1.57% false acceptance rate were achieved.**

***Index Terms*— Biometrics, continuous authentication, pattern recognition, electrocardiogram, local binary patterns.**

I. Introduction

PASSWORD is an intuitive approach to prevent unauthorized subjects from accessing a specific media. Usually after logging-in to a system with a password, the system would either be logged-in until the user logs-out, or the system logs-out the user after a 'grace period' of inactivity. Several gaps exist in such authentication process. Some scenarios illustrating the gap include: an intruder is able to access the system in the absence of the genuine user if the system is accessed within the session's grace period, and an intruder with the user's password is capable of accessing the system at any given time. As a result of these issues, research in continuous authentication (*hereafter CA*) systems has emerged. CA is referred to the task of continuously authenticating users while flagging intruders who attempt to access the system. There are several applications where CA can be utilized as a safeguard, such as computers [3], aircraft cockpits [4], cellphones, machines operating, cars, and other applications.

One stage towards achieving a robust CA system is by replacing the traditional authentication access methods (e.g. passwords and tokens) with biometrics, the field of study that models people's identity using their physical or behavioral traits [5]. For a CA system, it is desired to have a biometric system that does not require the cooperation of the subject (passive biometrics), cannot be spoofed, and available to all living human beings. Medical signals are viable candidates for such biometric systems. Some medical signals, namely Electromyogram (EMG) [6], muscle signal; Electrocardiogram (ECG) [7], heart electrical activities; and Electroencephalogram (EEG) [8], brain electrical signals were used as biometrics in the last decade. ECG is widely used and studied worldwide to diagnose heart problems, and it can be an inexpensive system to deploy.

ECG is recorded by attaching sensors to the body. This method of acquisition makes ECG biometrics superior to several other biometric systems where acquiring the biometric signal may distract the user. For example, face recognition, the user may need to look at the camera; fingerprint recognition, the user may need to swipe his/her finger; and speaker recognition, the user needs to speak. Another feature of ECG signal is that the signal is quasi-periodic; hence, observations are continuously available.

CA systems decide whether a subject is a genuine or an intruder subject by examining a pool of a classifier's outputs collected from several observations. Each classifier is fed by an observation, heartbeat in this paper; or a representation of the observation, feature extraction; and it outputs a decision confidence value (*hereafter confidence*). The class, genuine or intruder, on which an observation belongs to is decided based on the classifier confidence. In statistics, including machine

Manuscript received February 11, 2016; revised May 27, 2016 and July 15, 2016; accepted July 16, 2016. Date of publication August 10, 2016; date of current version October 11, 2016. This work was supported by the Natural Sciences and Engineering Research Council of Canada (NSERC). Parts of this paper regarding 1DMRLBP concept were proposed in 2014 19th International Conference on Digital Signal Processing and Canadian Conference on Electrical and Computer Engineering, [1], [2]. The associate editor coordinating the review of this manuscript and approving it for publication was Prof. PC Yuen.

The authors are with The Edward S. Rogers Sr. Department of Electrical and Computer Engineering, University of Toronto, Toronto, M5S 3G4, Canada (e-mail: wlouis@ece.utoronto.ca).

Color versions of one or more of the figures in this paper are available online at http://ieeexplore.ieee.org.

Digital Object Identifier 10.1109/TIFS.2016.2599270

learning, the term garbage-in garbage-out is well understood, undesired output is produced when an unrepresentative input is supplied. Therefore, having undiscriminating features that do not have small intraclass variation and large interclass variation among subjects jeopardize the CA system performance.

Many challenges are encountered while processing ECG signal as biometrics. There are several sources for signal artifacts that interfere with ECG acquisition. EMG interference is an electrical signal due to muscles contractions. Power line interference, on the other hand, interferes at 50Hz or 60Hz. Furthermore, due to respiration, a baseline wander of 0.15-0.30Hz [9] interferes with ECG signals. Also, contact noise affects the signal in the range from 1-10Hz. Another challenge is dealing with observations collection speed. ECG signal usually has a period frequency of 1-1.5 heartbeat/second. It is a slow signal if compared to another type of biometric system such as video face recognition that may stream at a rate of 30 frames/second. As a result, in a specific time-frame, significantly less number of observations are collected from ECG signal than from a video of faces. The challenge here is that if we require 100 observations to train a classifier, then we need around 3 minutes of ECG signal data acquisition, which may not be possible. Similar issue persists when the biometric system makes a decision from observations. Therefore, designing an ECG biometric system requires a system that can make a reliable decision using small sample size. Finally, ECG signal variates due to physiological and psychological changes, and it changes due to activity, diet [7], diseases, positions of the electrodes [10], and other factors. Proper techniques and feature selections are usually applied to overcome these challenges.

It is desired to design a robust ECG biometric system that can detect and flag intruders continuously. We propose One Dimensional Multi-Resolution Local Binary Patterns, 1DMRLBP. These features are inspired by the image based Local Binary Patterns (LBP) [11], yet they are modified and enhanced to be applicable to 1D signals; to tolerate quantization error and noise, in particular, noise that causes shifting and scaling of ECG signal, and noise due to signal segmentation misalignment; to preserve ECG heartbeats morphology; and to account for ECG signal temporal variations through an extraction mechanism. Furthermore, 1DMRLBP features type is an online feature extraction in a sense that it can be applied in real-life scenarios, and it depends on past observations only. A conventional method to implement a CA system is that the designer pre-allocates a segment size that corresponds to the number of confidences the CA needs in order to make a decision. The designer also pre-sets decision thresholds to decide on the class of the subject from each segment of confidences. In this work, we propose a novel method that allows us not to pre-allocate segment size and decision thresholds. This contribution uses sequential sampling to achieve a CA system that utilizes 1DMRLBP features properties. Together, 1DMRLBP and sequential sampling, constructs a CA system that dynamically adjusts segment size and decision thresholds while the biometric system keeps collecting input data.

This paper is organized as follows: Section II reviews literature in ECG biometrics and in CA. Section III presents filtration, classification, and the proposed 1DMRLBP and CA. Section IV describes the examined databases and the method of evaluation. Section V provides experiments and results. Section VI concludes this work. Lastly, the Appendix section compares the proposed feature extraction to other related feature types from the literature.

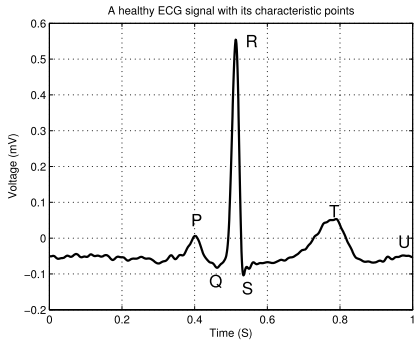

Fig. 1. ECG signal illustrating the main characteristic points.

II. Literature Review

This section presents the state of the art for 1) ECG signals as a biometric system and 2) CA systems.

A. ECG as Biometrics

One of the earliest works that examined ECG for biometric systems dates back to 1977 [12]. However, the need for biometric systems using biomedical signal did not catch much attention until the millennium [13]. In general, healthy ECG heartbeat has six characteristic or fiducial points, namely P, Q, R, S, T, and U. These points are illustrated in Figure 1. Based on these fiducial points, two mainstreams of ECG analyses have been proposed in the literature: fiducial and non-fiducial points based approaches. ECG heartbeats are isolated from ECG signals then aligned together to have a persistent feature extraction. Most of the techniques, whether they are fiducial or non-fiducial points based approaches, perform heartbeat isolation and alignment. Some exceptions exist such as the works in [14]–[16]. In fiducial points based approaches, features are extracted from fiducial points. Features can be distances between points, angles, areas, amplitudes, etc. One of the most pertinent works to this paper in the fiducial points based approach is in [17] because it deploys sequential sampling to make verification biometric decision. Multiple filtration stages were used as a first stage. Nine attributes extracted from fiducial points were considered as the features. These features were modeled as a multivariate Gaussian distribution. Decisions were made using sequential sampling criterion examining the claimed identity (null hypothesis) and the closest imposter identity (alternative hypothesis). Since non-fiducial points based approach is used in this paper, it is reviewed in more details.

Non-fiducial points based analysis technique is a holistic approach that considers the ECG signal or the isolated ECG heartbeat as a whole. Non-fiducial points based analysis can be further subdivided into two mainstreams: an approach that isolates and/or aligns the data as in [18] and [19] while the

other approach does not require any information about the signal as in [14], [16], and [20].

The approach in [21] applied Lyapunov exponents spectrum and correlation to capture the indexes of chaotic ECG signal. The research in [18] and [19] applied Discrete Wavelet Transform (DWT) directly to the raw ECG signal. The work in [22] detected and aligned P, QRS, and T waveforms then used wavelet distance measure for classification. While all mentioned techniques require heartbeat segmentation and/or alignment, the research in [16] is one of the earliest methods that does not require any information about ECG heartbeats. The authors acknowledged that there is no definitive and universally accepted rule about the onset and offset of an ECG heartbeat. In [16], auto-correlation (AC) was calculated on a window size of more than the duration of one heartbeat. The method in [23] is oriented in the same direction as [16]. Lastly, Ensemble Empirical Mode Decomposition (EEMD) in [24] was utilized for ECG biometrics.

B. Continuous Authentication (CA)

There are few papers on CA and ECG biometrics together. The work in [25] extracted QRS waveform from ECG signals and applied cross-correlation. Afterwards, several decision making strategies were experimented including *median*, *mean*, 75^{th} percentile, 90^{th} percentile, 95^{th} percentile, and *max* to obtain a single classification decision. The segment size, which is the number of samples (observations) needed to make a decision, was pre-determined. In [26], the research was fiducial based approach. It extracted 24 features from ECG heartbeats, used Mahalanobis distance for classification, then applied majority voting to make decisions on collected predefined size of observations.

The work presented in [14] used autocorrelation on an ECG signal then applied Linear Discriminative Analysis (LDA) for classification. Majority voting was used for decision making and continuous authentication. The research paper [27] applied a string matching technique based on Ziv-Merhav (ZM) cross-parsing [28]. In their CA system, the authors continuously updated the genuine subject model once a positive authentication occurred. These are papers that use both ECG and CA together.

Nevertheless, CA was examined for other biometric traits, especially keyboard keystroke and mouse movement, among others. The work in [29] examined mouse movement with different strategies and settings including static and dynamic trust model, fusion, and score boosting algorithms. In [30], mouse movements were examined as well. Neural Network was applied for classification, and sequential sampling was examined for CA. In [31], one class detector including Nearest-Neighbor detector, Support Vector Machine (SVM), and Neural Network were used. Segment size, in this case authentication time, was also pre-determined, and it showed that the longer the authentication period the higher the accuracy.

On the other hand, for keyboard CA systems, the work in [32] was trained by making users type predefined and frequently used words to generate a model. The algorithm was based on word by word decision. The score was compared to predefined thresholds, and a decision was made accordingly. Furthermore, a work similar to the work in [29] was applied to keystroke biometrics in [33]. The authors in [33] suggested a method to reduce the needed sample size by predicting a future desired probability from a smaller sample size.

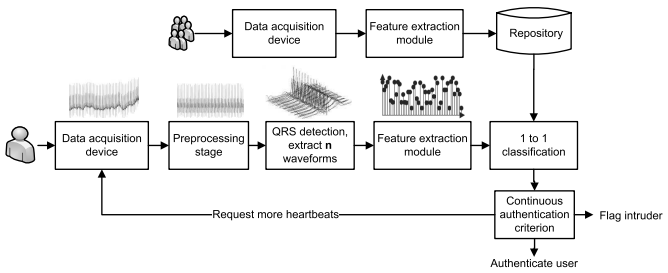

Fig. 2. Proposed CA system diagram.

Most, if not all, of the mentioned literature in ECG biometrics extract a feature vector for each observation independently, and these works do not consider the possible temporal changes among consecutive observations. Hence, a fusion and decision making stages are incorporated to make an identity decision from these observations. The literature of CA either uses multimodal biometrics or require a pre-set segment size (sample size or number of observations) and decision thresholds. These techniques cannot be used to achieve the objective of this paper, which is a CA system that does not require decision making strategy or fusion, and does not need a pre-set segment size and decision thresholds. For comparison purposes, we compared 1DMRLBP feature extraction to the AC/LDA [14] state-of-the-art work. On the other hand, for CA, the work in [30] by Ahmad *et al.* if adapted for ECG biometrics would be the closest study to compare our method to. Therefore it was adapted. Also, another comparison to state-of-the-art CA system by Labati *et al.* [25] was conducted.

III. Methodology

To develop an ECG biometric CA system that is highly accurate, and can adaptively decide on the number of observations and accept/reject decision thresholds, this paper proposes a unique CA strategy and technique by using sequential sampling and 1DMRLBP features.

This paper also proposes 1DMRLBP that can be effectively utilized with sequential sampling. 1DMRLBP is fast to extract, extracts ECG discriminative features, extracts observations temporal variation, and has the capability to transfer n ECG heartbeats into 1 feature-space vector using a merging mechanism. 1DMRLBP is classified using Bootstrap Aggregating (bagging) [34]. After classification, sequential sampling assists in constructing a CA system and decides whether to make a final identity decision or to ask for more observations. Figure 2 illustrates the overall system design.

A. Preprocessing Stage

ECG signal spans the frequencies between 0.05-40Hz [23]. Other works claim that ECG signal spans useful frequencies up to 100Hz [9]. Similar to [23] and [35], a fourth

order band-pass Butterworth filter with cutoff frequencies of 1-40Hz was applied. With this filter, baseline wander and higher frequencies of power line interference were reduced.

Heartbeats were isolated and aligned based on their R peaks. Pan-Tompkins procedure [36] was used for this task. The isolated heartbeat was 1 second duration and was centered at the R peak. Several works, including [37]–[39], align ECG heartbeats based on R peaks.

B. Feature Extraction

1DMRLBP feature extraction is an adaptation, a modification, and an advancement of the two dimensional image based Local Binary Patterns (LBP) [11] to suit one dimensional (1D) ECG signals. We first introduce background research about works that attempted transferring LBP features into One Dimensional Local Binary Patterns (1DLBP) features then we propose 1DMRLBP.

1) Review of One Dimensional Local Binary Patterns (1DLBP): Work to apply LBP for 1D signal was proposed in [40]. Other studies have also applied the work of [40] for 1D signal as in [41] and [42]. In [41], the authors utilized 1DLBP on a 1D signal; however, the authors in [42] applied 1DLBP to 2D images after projecting the images into 1D space. The work in [40] extracts binary patterns (BP) of time-sample $x(t)$ as:

$$BP(x(t)) = \sum_{i=0}^{p-1} sign(x(t+i-p) - x(t))2^i + sign(x(t+i+1) - x(t))2^{i+p} \quad (1)$$

Where t is the time index of the heartbeat, p is the number of points (time-samples) to be considered on each side of $x(t)$, and $x(t)$ is the time-sample that 1DLBP is desired to be extracted for. Also, $sign(.)$ is defined as the following:

$$sign(x) = \begin{cases} 1 & \text{if } x \geq 0 \\ 0 & otherwise \end{cases} \quad (2)$$

All proposed 1DLBP features in [40]–[42] used one specific BP resolution. The 1DLBP feature vector is the distribution of these BP values.

2) One Dimensional Mutli-Resolution Local Binary Patterns (1DMRLBP): 1DMRLBP preserves texture of multiple time domain signals in one feature vector. Like 1DLBP and LBP, 1DMRLBP captures and encodes the shape of an ECG signal using binary patterns. Unlike 1DLBP, LBP, and most of their variations in the literature, 1DMRLBP extracts a feature vector that captures temporal changes of observations, and it has a mechanism to merge n time domain heartbeats into 1 feature vector such that:

$$1DMRLBP(x(t)) : \{x(t) \in \mathbb{R}^{k \times n}, 1DMRLBP(.) \in \mathbb{Z}^m\} \quad (3)$$

where n is number of heartbeat samples, k is dimensionality of a time domain heartbeat sample, and m is the dimensionality of a feature vector. Subsequent sections, in particular Algorithm 1, explains the transformation mechanism of Equation (3) that changes n observations into 1 feature vector.

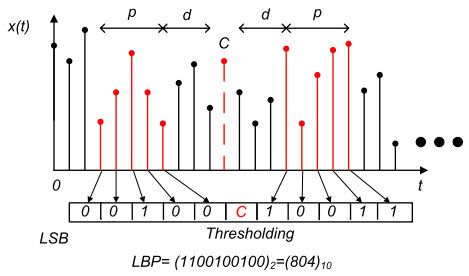

Fig. 3. Multi-resolution BP with $d = 4$, $p = 5$.

Extracting 1DMRLBP is a low computational complexity operation; hence, it can be implemented in low power devices. The features and properties of 1DMRLBP are:

a) 1DMRLBP accounts for quantization error: In 2D images, pixel values have a known range (e.g. [0,...,255] in the case of gray scale image); hence, Equation (2) performs well when used. In such case, the influence of step size is known (i.e. the difference between two consecutive levels is numerical 1 with a maximum difference of 255). In ECG signal, however, that's not the case, and this is an issue. Despite quantization level for the acquisition instrument could be known, the highest peak of the ECG signal stays unknown. Consequently, Equation (2) might not be adequate to capture the morphology of an ECG signal. Equation (2) is modified by adding a leeway in binary patterns extraction to accommodate such issue. A parameter, ϵ, is included in Equation (4) to account for quantization error. Also, adding this leeway reduces the influence of ripples (noise) on ECG signals.

$$sign(x) = \begin{cases} 1 & \text{if } x + \epsilon \geq 0 \\ 0 & otherwise \end{cases} \quad (4)$$

b) 1DMRLBP captures multiple resolutions: Unlike 1DLBP in [40] and [42], 1DMRLBP does not capture texture based on fixed number of points only. It considers different distances, d, and points, p, where d is how far from the desired time-sample, $x(t)$, the features start to get extracted, and p is how many time-samples are considered for 1DMRLBP feature extraction from each side. Figure 3 demonstrates the multi-resolution concept.

$$BP(x(t)) = \sum_{i=0}^{p-1} sign(x(t+i-p-d+1) - x(t))2^i + sign(x(t+i+d) - x(t))2^{i+p} \quad (5)$$

Where $sign(.)$ is as in Equation (4). $BP(x(t))$ is assigned to a value of zero when its parameters require information that is out of boundaries. It becomes out of boundaries when $t+i+d > k$, where k is the heartbeat length, and when $t+i < p+d$. From Figure 3, with different p and d, multiple resolutions can be captured for the same time-sample. Such structure retrieves more signal characteristics than single resolution. Up to this point of the discussion, the 1DMRLBP as in [1] does not have the capability to capture the changes occur to ECG signal over time.

Algorithm 1 1DMRLBP Feature Extraction

Data: $\boldsymbol{X} \in \mathbb{Z}^{k \times n}$, binary patterns for n observations
Δ, windows shifting steps, w, windows sizes
Result: $\boldsymbol{x} \in \mathbb{Z}^{m \times 1}$, 1DMRLBP
Start with first observation $i = 1$, first window $j = 1$, and an empty feature vector of the 1DMRLBP=[ ];
Calculate l, number of windows, $l = 1 + \lfloor \frac{k-w}{\Delta} \rfloor$;
while $j \leq l$ **do**
  Initiate $S_j \leftarrow [\ ]$;
  while $i \leq n$ **do**
    $S_j \leftarrow w_{i,j}$, the j^{th} window in the i^{th} observation;
  end
  1DMRLBP$_j \leftarrow$ distribution of (S_j) ;
  Normalize 1DMRLBP$_j$;
end
return *Concatenate* $(1DMRLBP_j)_{j=1}^{l}$ *for all windows*

c) 1DMRLBP considers temporal changes: In most variants of LBP, 1DLBP, and earlier stages of our work in [1], a feature vector is extracted from every observation. However, this is not the case for this paper's 1DMRLBP [2]. This paper's 1DMRLBP accounts for observations' temporal deviation through an algorithm that extracts one feature vector. This feature vector represents several consecutive observations that may undergo temporal changes. The advantage of this mechanism is that it results in one feature vector from multiple time-domain observations, and this characteristic is crucial for the CA system in this paper.

Some binary patterns works in the literature, especially image based LBP variants such as [43], [44], and others, have proposed extracting binary patterns features that capture temporal changes. Comparison between such approaches and the proposed 1DMRLBP is explained in Appendix VI.

1DMRLBP is desired to capture both local and global features of a signal. Also, it is preferred to have tolerance towards sparse noise and segments misalignment. Hence, similar to other LBP variants, BP values distribution is calculated.

To extract 1DMRLBP feature vector from n observations, first, BP is extracted for all n observations. Afterwards, we pre-assign overlapping and/or non-overlapping windows. The windows have two parameters, window size, w; and shift, Δ. At last, we apply the feature extraction mechanism that we propose in Algorithm 1 to extract one feature vector from n observations.

From the algorithm, it can be deduced that 1DMRLBP accounts for temporal changes of observations seamlessly without applying sophisticated fusion methods. The temporal changes extraction is achieved by modeling the distribution of binary patterns for a specific window from several consecutive observations. The result is always one feature vector. Since the feature extraction is based on finding the binary patterns distribution of each window over several observations, rather than finding the distribution from every single observation, then statistically this larger sample size leads to a more descriptive model, hence, higher accuracy in 1DMRLBP based biometric system. This is empirically proven in Section V-C. Extracting features using different window sizes allow

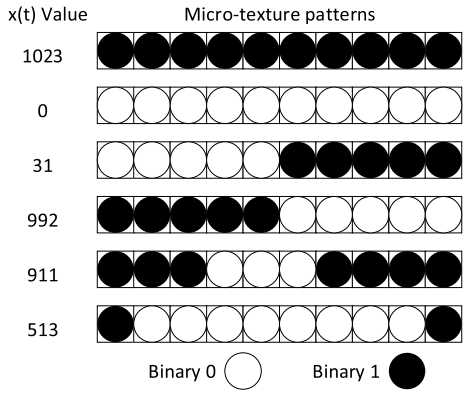

Fig. 4. An example of some micro-texture patterns that 1DMRLBP features capture.

1DMRLBP to capture both local and global features. Most, if not all, LBP variants calculate binary patterns distribution for each observation separately. This loses possible observations' temporal changes and produces a less descriptive distribution than 1DMRLBP because it is calculated from a smaller number of samples (i.e. one observation).

Through the stages that lead to the extraction of 1DMRLBP features, the discriminative power of this type of features is constructed by two stages: first, BP encodes the micro-texture of time-samples, $x(t)$. Micro-textures can be thought of as a template. The micro-textures have 2^p patterns, and they capture edges, flat areas, or special pattern as in Figure 4. Second, frequency of these patterns from local and global windows within the same observation, and frequency of the patterns through multiple observations emphasize on specific patterns of a subject, thus, increase 1DMRLBP discriminative power.

d) 1DMRLBP achieves robustness towards noise: Throughout the explained sections on the parts that comprise 1DMRLBP features, theoretically, these features can tolerate noise due to their method of extraction. Apart from quantization error, noise that causes shifting and scaling of the signal, signal segmentation misalignment, and other noise that may defect some heartbeats are other issues that 1DMRLBP can tolerate. Similar concept to [11], we capture micro-texture patterns, M, revolving around each time-sample, $x(t)$, and we do that by calculating the joint distribution of the micro-texture patterns, m, for all p points in the 1DMRLBP. Let $k = 1 - p - d$, then we have

$$M(x(t)) = m(x(t), x(t+k), x(t+1+k), \ldots, x(t+p-1+k)) \quad (6)$$

Shift invariance is achieved by subtracting the time-sample, $x(t)$, from neighboring time-samples. So the distribution becomes:

$$M(x(t)) = m(x(t), x(t+k) - x(t), x(t+1+k) - x(t), \ldots, x(t+p-1+k) - x(t)) \quad (7)$$

We assume the term $x(t)$ as carrying just the level or the average value of the micro-texture of that time-sample and no micro-texture information. So it is independent of the terms

$x(t+i+k)$, where $i \in 0, 1, \ldots, p-1$. Therefore, we can factor it out [11]. As a result, the distribution becomes:

$$M(x(t)) = m(x(t))m(x(t+k)-x(t), \ldots, x(t+1+k)-x(t), x(t+p-1+k)-x(t)) \quad (8)$$

Next, $M(x(t))$ is approximated by omitting the independent term $m(x(t))$. The micro-texture of $x(t)$, $M(x(t))$, is:

$$M(x(t)) \approx m(x(t+k)-x(t), x(t+1+k)-x(t), \ldots, x(t+p-1+k)-x(t)) \quad (9)$$

Despite the fact that the distribution is approximated, doing so achieves shift invariant features. To construct scaling invariant features, Equation (4) is applied to every term in Equation (9). With the explained steps thus far, 1DMRLBP features are invariant to noise that causes shifting and scaling, and it can tolerate quantization error.

The micro-texture, $M(x(t))$, has a binary value, which is encoded into a decimal value. This is the binary pattern, BP, of a sample. Instead of classifying each BP by itself as in [45], we applied histogram on overlapping and/or non-overlapping windows. Histogram does not only capture morphological information, but it eliminates spatial information, hence, reduces misalignment error that may arise due to noise interference or signal segmentation error. Lastly, we capture the distribution of multiple observations using Algorithm 1. Such step captures temporal variation among ECG signals and reduces the effect of abnormal ECG heartbeats that may appear between normal heartbeats.

To summarize 1DMRLBP contributions and properties:

- Unknown signal amplitude, quantization error, shifting, scaling, and misalignment issues are tolerated.
- To extract 1DMRLBP, four parameters are needed d, p, w and Δ.
- Different combinations of d and p capture different feature-space resolutions.
- 1DMRLBP has a mechanism to extract temporal changes from observations, and it captures local and global morphological features. These properties along with sequential sampling construct the CA system proposed in this paper.

C. Classification

There are several classification methods in the literature, and bagging [34] is one of them. In a nutshell, bagging is a machine learning technique that generates weak classifiers/predictors. The aggregated average of weak classifiers makes a decision. We used bagging in particular because we observed an unstable classifier prediction when we examined ECG heartbeats data. It is unstable in a sense that slight change in the training data led to a significant change in the construction of the classifier and a significant change in accuracy. Bagging usually reduces this issue [34]. Comparison to other classifiers, SVM [46] and single decision tree, are presented in Section V-A.1.

Suppose a training dataset, $\mathcal{L}$, is populated with data $\{y_n, \mathbf{x_n}, n = 1, \ldots, N\}$, where y is the data class and $\mathbf{x}$ is the input data. From these samples, bagging generates multiple bootstrap samples, $\mathcal{L}^{(B)}$, from $\mathcal{L}$. For each $\mathcal{L}^{(B)}$, it finds a predictor, $\phi(\mathbf{x}, \mathcal{L}^{(B)})$, that predicts the class, y. Bootstrapping samples, $\mathcal{L}^{(B)}$, are constructed by drawing N samples with replacement from $\mathcal{L}$. The predictor used in this paper is simple decision tree. The final decision on the class is made by voting.

D. Sequential Sampling

Conventionally, CA systems use a predefined number of observations along with a pre-set decision threshold to make a positive (authenticate) decision or a negative (reject) decision. Setting the number of observations and decision threshold parameters has a trade-off between accuracy and time. Hence, a method that can avoid setting these parameters is desired. For such purpose we examined sequential sampling [47].

Sequential sampling is a statistical approach that follows criteria to accept a hypothesis, reject a hypothesis, or ask for more samples to decide. In a similar manner, we use sequential sampling for ECG signal CA system such that the three criteria are: *authenticate region*, *reject region*, and *continue region*. Along with these criteria, we propose using "segments". The onset of the first segment is on the first observation tested while the offset is when a decision is made. The second segment onsets on the first observation after the offset of the previous segment, and so on. The temporal information for observations are extracted using 1DMRLBP for the duration of each segment only.

During operation, when *authenticate region* criterion is met (positive authentication), it means a genuine person is providing his/her signal. Hence, CA system ends the current segment and initiates another one. On the other hand, when *reject region* criterion is met (negative authentication), it means an imposter (intruder) has provided his/her signal. Therefore, CA ends the segment and flags the signal provider as an intruder. Lastly, when CA is in *continue region*, it means a bigger sample size is needed. Figure 10 illustrates real-life continuous authentication system in action using sequential sampling. It shows 14 segments where each segment has its criterion getting updated progressively as the segment's sample size increases. Figure 10 also shows the segment re-initialization once a criterion is met. The upper lines represent the minimum classification confidence to accept a sample while the lower lines represent the minimum classification confidence in order not to reject a sample. As the number of samples increases, the acceptance and rejection thresholds change accordingly (upper and lower lines in Figure 10, respectively). Unlike traditional works, an acceptance/rejection threshold is not set.

The main advantage of sequential sampling is that it is optimized to minimize the sample size needed to make a decision. Sequential sampling has two alternative hypotheses where each hypothesis is a one-sided hypothesis. When a sample is not significantly different from both hypotheses, a decision cannot be made and more observations are needed. Since a single confidence value is needed to check significance from the hypotheses, then the usefulness of the property of 1DMRLBP that achieves one feature vector from multiple observations becomes crucial in this stage. One of the sequential sampling

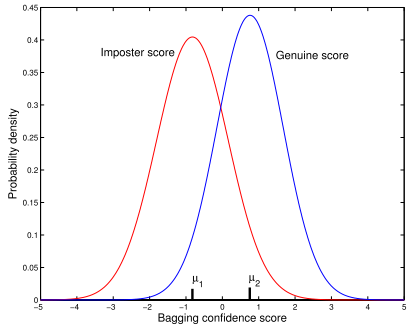

Fig. 5. Genuine and imposter distances distributions.

conditions is that the data should be drawn from a binomial distribution. The hypotheses for the sequential sampling are constructed from two distributions: genuine confidences and imposter confidences. Figure 5 illustrates the hypotheses.

The parameters that control the sequential sampling criteria are: Type I error, α, Type II error, β; and the hypotheses means, μ_1, μ_2 for the imposter and genuine scores distributions, respectively. On segment onset, the alternative hypotheses are set as in Equation (10) [48]:

$$\begin{aligned} H1 &: \text{classification distance} \geq \mu_1 \\ H2 &: \text{classification distance} \leq \mu_2 \end{aligned} \tag{10}$$

Setting up α and β is setting up risks such that α corresponds to the risk of rejecting H_1 and accepting H_2 while the sample belongs to H_1. Similarly, β corresponds to the risk of rejecting H_2 and accepting H_1 while the sample is actually from H_2.

After setting up the hypotheses, the decision criteria need to be updated based on the number of samples observed. The criteria are represented by the parallel lines separating the regions as seen in Figure 10. The equations for the lines are as in Equation (11).

$$\begin{aligned} \text{Upper Line (UL)} &: Y = bn + h_1 \\ \text{Lower Line (LL)} &: Y = bn + h_2 \end{aligned} \tag{11}$$

The slope, b, can be calculated as $b = \frac{\mu_1+\mu_2}{2}$. The y-intercept can be calculated from the following two equations [48]:

$$h_1 = \frac{B\sigma^2}{\mu_1 - \mu_2}, \quad h_2 = \frac{A\sigma^2}{\mu_2 - \mu_1} \tag{12}$$

Where $A = \log\frac{1-\alpha}{\beta}$, and $B = \log\frac{1-\beta}{\alpha}$. σ is the standard deviation of the distances. To compute the decision up to observation n, c_n, and check whether it meets any of the criteria then Equation (13) is used.

$$C_n = \sum_{1}^{n} c(n) \tag{13}$$

$c(n)$ is the classification confidence for 1DMRLBP feature vector, which is calculated using Algorithm 1 for sample n. It is worth mentioning that the wider the undecided area (the area between the lines in Figure 10) the more aggressive the criteria are. By aggressive we mean more observations are needed to make a decision. The closer the means are in the hypotheses, Figure 5, the more aggressive the criteria are. Same concept applies to α and β such that the smaller the number the more aggressive the criteria are.

IV. Experimental Set Up

Several databases are available for ECG analyses; however, most of these databases are collected and dedicated for medical applications. This section presents the examined databases and lay down the method of evaluation used to examine the proposed system.

A. University of Toronto Database (UofTDB)

This database was collected at the University of Toronto [49]. It was collected in 6 sessions that spanned a 6-month period. Not all subjects were involved in all 6 sessions. UofTDB was recorded from fingertips with single lead. The sampling rate for the signal is 200Hz. This database has 1,020 subjects. Out of the 1,020 subjects, 1,012 subjects had come in the first session, 82 subjects had come twice, and out of the 82 subjects, 43 subjects had come for the 6 sessions. For this paper, we considered single and multiple sessions subjects, $1,012$ and 82 subjects, respectively.

We constructed the training and testing datasets as follows: in the multiple sessions experiment, one session from each subject was used as genuine training dataset and the other session(s) for that subject were used as genuine testing dataset(s). This was repeated for every session and every subject. In other words, every session for every subject was once treated as genuine training dataset and in other times as genuine testing dataset. The other 81 multiple sessions subjects formed the imposter testing dataset. The imposter training dataset to train the classifier was randomly drawn from subjects that did not belong to the 81 multiple sessions subjects. In single session experiments, the first 80% of each subject's heartbeats were used as genuine training dataset while the other 20% were used as genuine testing dataset. Subjects randomly drawn from the other 1,011 subjects constructed imposter training dataset. The other subjects that were not part of the imposter training dataset created the imposter testing dataset.

Heartbeats from fingertips are susceptible to noise. In order to remove outliers, Interquartile Range (IQR) [50] for R peaks for ECG heartbeats was calculated. The heartbeats were isolated as explained in Section III-A. Statistically, $IQR = Q_3 - Q_1$, where Q_3 corresponds to 75^{th} percentile while Q_1 corresponds to the 25^{th} percentile. Outliers limits are defined as:

$$\begin{aligned} U_{outlier} &= Q_3 + 1.5 \times IQR \\ L_{outlier} &= Q_1 - 1.5 \times IQR \end{aligned} \tag{14}$$

Heartbeats with R peak amplitude greater than $U_{outlier}$ or less than $L_{outlier}$ were considered as outliers and were removed.

B. PTB Database

A publicly available database called the PTB Diagnostic ECG Database [51] was also used. This database was collected

from healthy and non-healthy subjects and is usually used for medical diagnosis. The non-healthy subjects suffer from different heart related diseases. This database was recorded using 12-lead ECG configuration and three Frank leads. Each ECG signal is sampled at 1KHz. The database has 549 records from 290 subjects. The database has 52 healthy subjects. Out of the 52 subjects, 14 subjects have more than one recording. Some of these multiple recordings are several years apart. Heartbeats were isolated and healthy and non-healthy datasets were constructed for experimentation.

C. Method of Evaluation

Performance Rate (PR), False Acceptance Rate (FAR), False Rejection Rate (FRR), number of Genuine Observations (GO), number of Intruder Observations (IO), Receiver Operating Characteristic (ROC) curve, and Equal Error Rate (EER), were the main measures used in this paper. Each examined dataset has $G + I$ samples, with G is being the number of *genuine* samples (observations), and I is being the number of *imposter (intruder)* samples.

We define number of true positive, nTP, as the number of correctly classified genuine samples. Similarly, the number of true negative, nTN, is defined as the number of correctly classified imposter samples. Moreover, number of false positive, nFP, is the number of misclassified imposter samples as genuine samples. Likewise, the number of false negative, nFN, is the the number of misclassified genuine samples as imposter samples. Following these definitions,

$$FAR = \frac{nFP}{I}, \quad FRR = 1 - \frac{nTP}{G}, \quad PR = \frac{nTP + nTN}{G + I} \tag{15}$$

Despite the fact that PR might seem the most appealing quantity since it includes all measures, all quantities in Equations (15) should be considered as PR would be misleading when $I \gg G$ or $I \ll G$.

GO is the average number of observations needed to reach a decision in a CA segment when a genuine person is examined. On the other hand, IO is the average number of observations to reach a decision in a CA segment when an imposter person is examined. Quantities similar to GO and IO were used and reported in [29]. ROC curve measures the performance of a system in different operating points. ROC curve plots FRR versus FAR. Closely related is EER. EER is the error on the operating point on which $FAR = FRR$.

Lastly, the terms *training error* and *testing error* are usually used in machine learning literature. The term *training error* is called on the error resulted when examining classifiers on training set. However, *testing error* is called on the error resulted when examining classifiers on testing set.

V. Experimentation

A. 1DMRLBP as a Feature Extraction

The capability of using 1DMRLBP for ECG analysis was examined on two databases for two different applications to show that 1DMRLBP is not restricted for a single application or a database. The applications are medical and biometrics applications. In the medical application [1], classification of healthy versus non-healthy ECG heartbeats were conducted on the PTB database. For the biometrics application, 1DMRLBP was examined on UofTDB for a verification biometric system. A verification biometric system is a binary pattern recognition problem where the output is to accept or reject a claimed identity. A verification system was designed since it is a required stage in a CA system which needs to verify the identity of a person or to flag the person as an intruder.

1) Experiment on PTB Database for Medical Application: In this experiment, 1,000 healthy ECG heartbeats and 1,000 non-healthy ECG heartbeats randomly selected from the database were used to train classifiers. All 1DMRLBP feature vectors were extracted as explained in Algorithm 1. The number of observations in the algorithm was set to $n = 1$ because neither CA nor observation temporal consideration were desired to be examined in this experiment. The classifiers in Section III-C were deployed. By setting the operating threshold of choosing between classes (healthy and non-healthy) to 50%, the results are tabulated in Table I.

It can be observed that p was set to 4 in most cases in Table I. The parameter p controls the number of histogram bins for each window. Number of histogram bins is $2^{2\times p} = 256$ bins for each window. The reason to slightly lower results when $p = 5$ is associated with the need for more training data than that when $p = 4$ since $p = 5$ has a feature vector of 10,240 features in comparison to 2,560 features when $p = 4$. However, when we examined a smaller p value, $p = 2$, the result did not change dramatically, but the feature vector was significantly reduced to 160 features. We used two sets of parameters throughout this work: $d = (100, 200)$, $p = (4, 4)$, $\Delta = (100, 200)$, $w = (500, 400)$, and $d = (100, 200)$, $p = (2, 2)$, $\Delta = (100, 200)$, $w = (500, 400)$. These parameters are relative to ECG heartbeat length, k. They can be presented as a proportion to k so they can be applicable to other signals with different sampling rate. For example, PTB heartbeats have 1,000 samples per heartbeat because the heartbeat is sampled at 1KHz, and we considered each heartbeat to span one second as explained in Section III-A. When $d = (100, 200)$, $p = (4, 4)$, $\Delta = (100, 200)$, $w = (500, 400)$, and $d = (100, 200)$, $p = (2, 2)$, $\Delta = (100, 200)$, $w = (500, 400)$, the parameters can be expressed as $d = (0.1 \times k, 0.2 \times k)$, $p = (4, 4)$, $\Delta = (0.1 \times k, 0.2 \times k)$, $w = (0.50 \times k, 0.4 \times k)$, and $d = (0.1 \times k, 0.2 \times k)$, $p = (2, 2)$, $\Delta = (0.1 \times k, 0.2 \times k)$, $w = (0.50 \times k, 0.4 \times k)$, respectively. As can be seen from Table I, these parameters achieved the highest performance.

The following explains how the feature vector length of 2,560 was constructed. In case of $d = 100, p = 4, \Delta = 100, w = 500$, we have 6 windows calculated using $l = 1 + \lfloor \frac{k-w}{\Delta} \rfloor$. Each window has $2^{2\times p} = 256$ bins. Windows' feature vectors are concatenated to have $6 \times 256 = 1,536$ features. Furthermore, in the next resolution when $d = 200, p = 4, \Delta = 200, w = 400$, there are 4 windows with 256 features for each window. All windows are concatenated to achieve $4 \times 256 = 1,024$ features. The total is $2,560$ features per feature vector.

It can be noticed from Table I that SVM has significantly worse performance than bagging. SVM with Gaussian Radial

TABLE I

1DMRLBP CAPABILITY TO CLASSIFY ECG HEARTBEATS. MULTIPLE RESOLUTIONS ARE READ RESPECTIVELY, FOR EXAMPLE $p = (4, 4)$ AND $d = (100, 200)$ MEANS $p = 4$ AND $d = 100$, THEN AGAIN $p = 4$ AND $d = 200$

Classifier	points, p	distance, d	shift, Δ	window size, w	Feature vector length	FRR	FAR	PR
SVM	4	100	0	1000	256	0.52	0.06	0.83
SVM	4	50	0	1000	256	0.64	0.08	0.79
Bagging (no ϵ)	4	1	0	1000	256	0.29	0.34	0.68
Bagging ($\epsilon = 0.001$)	4	1	0	1000	256	0.17	0.23	0.75
Bagging ($\epsilon = 0.01$)	4	1	0	1000	256	0.09	0.17	0.84
Bagging ($\epsilon = 0.02$)	4	1	0	1000	256	0.27	0.13	0.83
Bagging ($\epsilon = 0.05$)	4	1	0	1000	256	0.36	0.25	0.71
Bagging (no preprocessing)	4	1	0	1000	256	0.24	0.28	0.73
Bagging	5	1	0	1000	1,024	0.18	0.28	0.74
Bagging	4	100	0	1000	256	0.18	0.19	0.82
Bagging	4	100	100	500	256	0.12	0.11	0.89
Bagging	4,4	1,100	0,0	1000,1000	512	0.14	0.14	0.86
Bagging	4,4	100,200	100,0	500,1000	1,792	0.11	0.17	0.90
Bagging	5,5	100,200	100,200	500,400	10,240	0.10	0.15	0.86
Bagging	4,4	100,200	100,200	500,400	2,560	**0.09**	**0.09**	**0.91**
Bagging	2,2	100,200	100,200	500,400	160	0.11	0.10	0.91
Single decision tree	4,4	100,200	100,200	500,400	2,560	0.15	0.14	0.86
SVM	4,4	100,200	100,200	500,400	2,560	0.01	0.96	0.07

Basis Function (RBF) was used. Data over-fitting and bias are some of the reasons that achieved the low performance since training error for SVM was 0% while testing error was significantly higher. Signal instability is another reason for the bad performance of SVM. Bagging performance is in Table I. The improvement of bagging over single decision tree was also experimented. Its result is also reported in Table I. This table clearly shows that bagging achieves better results than SVM and single decision tree.

The effect of modification by adding the leeway parameter ϵ in Equation (4) and the improvement due to the preprocessing stage are also noted in Table I. When we extract BP, we should consider that the ECG heartbeat might have some noise, and we do not want the noise to affect the extraction. Hence, we use Equation (4). This is an advantage over the hard binary patterns extraction in most LBP feature variants that are based on Equation (2). The value ϵ should not be of a high value such that it can conceal signals features. We chose ϵ of a value proportional to the standard deviation of the examined signals; e.g. 10% of ECG signals standard deviation was ≈ 0.001. Table I reports experiments with ϵ values of $0.001, 0.01, 0.02$, and 0.05.

2) Experiment on UofTDB for Biometrics Application: After examining 1DMRLBP's capability to extract ECG discriminative feature for medical application, it was experimented for a verification biometrics application. First part of this experiment examined 1DMRLBP parameters choice. It was experimentally discovered that the best results among the examined parameters were achieved using the same parameters that resulted in the highest performances in Section V-A.1. This experiment also showed that having different resolutions affect the result, and this is plotted in Figure 6. In Figure 6, the highest performing two sets of parameters achieved almost identical accuracy; however, the set of parameters with $p = (2, 2)$ produced a feature vector of dimensions that is only 6.25% of that with the parameters using $p = (4, 4)$.

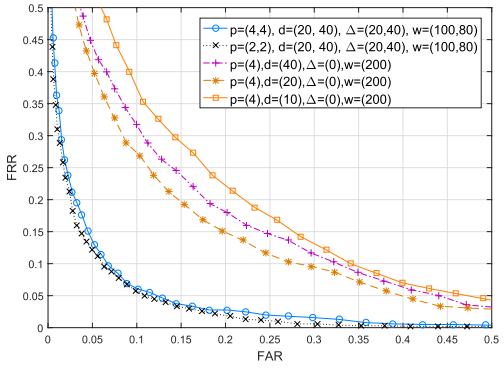

Fig. 6. 1DMRLBP in a verification biometric system.

To prove the capability of 1DMRLBP to perform well for biometrics purposes, two types of experiments were designed for the task: one experiment used one session subjects in order to utilize the whole database of 1,012 subjects, hence, ensure scalability in lower variance in performance and compare to state-of-the-art method that examined single session. The other experiment considered subjects with multiple sessions (82 subjects) to illustrate 1DMRLBP's capability to be applied in real-life situations and to avoid possible classifier bias. The training and testing datasets are non-overlapping and their construction is discussed in Section IV-A. Figure 6 reports the ROC curves for 1,012 single session subjects biometrics experiment. Multiple sessions experiment was conducted, and its results was compared to single session experiment. Figure 7 illustrates this result. After presenting that 1DMRLBP performs well on multiple sessions database, the experiments onward will be diverted back to single session to obtain a robust results based on 1,012 subjects.

To summarize the outcomes of this experiment:

- 1DMRLBP is capable of extracting ECG heartbeat discriminative features.
- Multi-resolution increased performance accuracy by 16%.

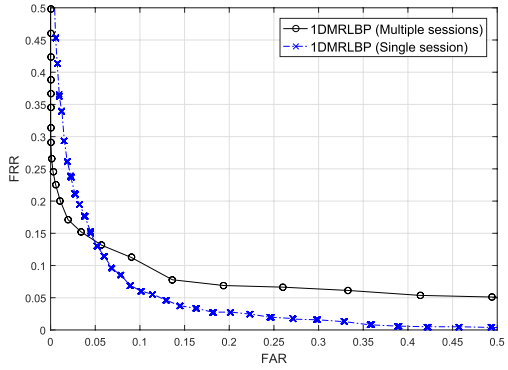

Fig. 7. Multiple sessions versus single session experiment. EER for single session is 7.89% and for multiple sessions is 10.10%.

- Ensemble classifier with decision tree achieved higher accuracy than SVM and single decision tree.
- Preprocessing increased accuracy by 7% FRR, 5% FAR, and 2% PR in comparison to the experiment without preprocessing that had $FRR = 24\%, FAR = 28\%, PR = 73\%$.
- The modified $sign(.)$ with $\epsilon = 0.001$ in Equation (4) improved the result by 12% FRR, 11% FAR and 7% PR in comparison to the experiment that did not use ϵ in the $sign(.)$ which had $FRR = 29\%, FAR = 34\%, PR = 68\%$.
- 1DMRLBP can be applied for biometrics applications. It achieved an EER of 7.89% on 1,012 single session database and an EER of 10.10% on 82 multiple sessions database.

B. 1DMRLBP Features Contribution to Accuracy

We desired to investigate whether 1DMRLBP feature type has a substantial contribution in improving accuracy of a biometric system, and it is not due to other factors only such as the bagging classifier. Therefore, two biometric systems were compared. In both systems, bagging classification was not used, and Euclidean distance was utilized instead. One system implemented 1DMRLBP features, and the other system used same set of heartbeats but without 1DMRLBP, in other words it used raw time-samples. The parameters in Section V-A.1 that yield 2,560 dimensions feature vector were used in the biometric system that utilized 1DMRLBP features. The raw time-samples has feature vectors of 200 samples. Principal Component Analysis (PCA) with number of components that achieved small performance variance across subjects in the raw time-samples was selected. Ten components were chosen. Same number of components was used for PCA with 1DMRLBP to have the same feature vector length as that in raw time-samples after PCA projection. The advantage of 1DMRLBP is apparent from Table II with an improvement of 15% in EER.

C. Capability and Advantage of Temporal Variation Extraction

The 1DMRLBP feature extraction capability to capture observations' temporal changes using the mechanism explained in Algorithm 1 was compared to 1DMRLBP where temporal variation extraction was not exploited i.e. Algorithm 1 with $n = 1$.

TABLE II
1DMRLBP FEATURES CONTRIBUTION TO ACCURACY

Feature Type	Feature Reduction	Classification	EER(%)
1DMRLBP	PCA (10 feat.)	Euclidean	20.4
None	PCA (10 feat.)	Euclidean	35.8

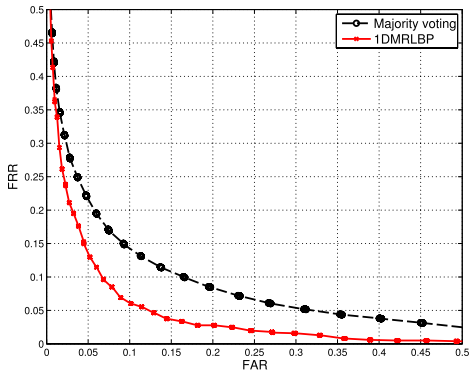

Fig. 8. 1DMRLBP with consideration to temporal variation versus 1DMRLBP without consideration to temporal variation among observations.

When temporal changes were not considered, majority voting decision-making scheme was deployed. No extra steps were required when 1DMRLBP utilized temporal changes extraction algorithm since the algorithm results in one feature vector. Figure 8 illustrates the comparison. Such experiment was conducted by fixing all other 1DMRLBP parameters. We can conclude that capturing observations' temporal changes improve biometric system accuracy.

D. Comparison to State-of-the-Art-Work ECG Biometrics

We compared the implemented biometric verification system to a state-of-the-art biometric verification system, AC/LDA [14]. AC/LDA biometric system does not require signal segmentation, and it uses autocorrelation (AC) as features. It applies LDA. Lastly, it uses Euclidean distance for classification. Figure 9 demonstrates the performance of 1DMRLBP using Algorithm 1 versus AC/LDA method.

Training to testing proportion of 80% to 20%, respectively, was used for AC/LDA. In AC/LDA, majority voting was used for the decision making while that was not needed for 1DMRLBP. For heartbeats outliers elimination, IQR elimination as explained in Section III-A was utilized in 1DMRLBP, while autocorrelation coefficient based outlier removal was used in AC/LDA. IQR outlier removal is not applicable to AC/LDA since it requires the extraction of individual heartbeats, but AC/LDA is not based on isolated heartbeats. EER was calculated to be 7.89% for 1DMRLBP while it was calculated to be 12.30% for AC/LDA. From this experiment, we deduce that a biometric system based on 1DMRLBP is capable to outperform a state-of-the-art work.

E. Comparison to State-of-the-Art CA Systems and Influence of Sequential Sampling Parameters

A CA system was implemented using sequential sampling as explained in Section III-D. In the first experiment

TABLE III

SEQUENTIAL SAMPLING PERFORMANCE WITH DIFFERENT PARAMETERS AND COMPARISON BETWEEN SEQUENTIAL SAMPLING WITH 1DMRLBP FEATURES THAT CONSIDERS TEMPORAL VARIATION WITH 1DMRLBP THAT DOES NOT CONSIDER TEMPORAL VARIATION

	Parameters				1DMRLBP with temporal variation i.e. using Algorithm 1				1DMRLBP without temporal variation i.e. the work in [1]			
CA number	H_1 mean	H_2 mean	α	β	FRR	FAR	IO	GO	FRR	FAR	IO	GO
CA1	μ_1	μ_2	0.01	0.01	1.13%	8.11%	5.83	5.67	3.30%	9.10%	6.27	6.27
CA2	$\mu_1 - 0.1\sigma$	$\mu_2 + 0.1\sigma$	0.01	0.01	1.55%	8.98%	5.25	5.08	3.54%	9.95%	5.65	5.49
CA3	$\mu_1 - 0.3\sigma$	$\mu_2 + 0.3\sigma$	0.01	0.01	1.93%	9.68%	4.46	4.38	3.93%	8.14%	4.76	4.58
CA4	$\mu_1 + 0.1\sigma$	$\mu_2 - 0.1\sigma$	0.01	0.01	0.85%	7.51%	6.51	6.32	3.93%	8.14%	4.76	4.58
CA5	$\mu_1 + 0.3\sigma$	$\mu_2 - 0.3\sigma$	0.01	0.01	0.81%	5.94%	8.81	8.79	2.81%	7.24%	9.80	10.14
CA6	$\mu_1 + 0.4\sigma$	$\mu_2 - 0.4\sigma$	0.01	0.01	0.68%	4.82%	11.01	11.19	1.59%	5.71%	12.18	13.07
CA7	$\mu_1 + 0.6\sigma$	$\mu_2 - 0.6\sigma$	**0.01**	**0.01**	**0.39%**	**1.57%**	**30.10**	**34.38**	0.92%	3.17%	34.50	40.40
CA8	μ_1	μ_2	0.001	0.001	0.56%	6.77%	7.70	7.74	1.26%	7.27%	8.52	8.75
CA9	μ_1	μ_2	0.0001	0.0001	0.60%	5.47%	9.36	9.25				
CA10	μ_1	μ_2	0.01	0.001	0.32%	9.33%	7.71	5.80				
CA11	μ_1	μ_2	0.001	0.01	0.89%	6.22%	5.91	7.80				
CA12	μ_1	μ_2	0.1	0.01	1.41%	12.03%	5.61	3.56				
CA13	μ_1	μ_2	0.01	0.10	3.30%	7.386%	3.71	5.40				

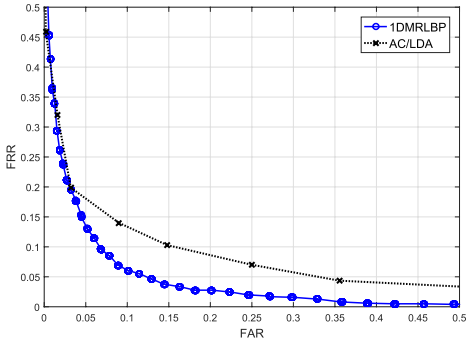

Fig. 9. 1DMRLBP versus AC/LDA [14].

of this subsection, this paper's CA system was examined for biometric application on UofTDB and was compared to other two CA systems of Ahmed and Traore [30] and Labati *et al.* [25]. In the second experiment, we compared two 1DMRLBP based CA systems, one was based on 1DMRLBP that extracted temporal variation and used sequential sampling to one that was based on 1DMRLBP that did not deploy temporal variation extraction [1] (i.e. $n = 1$ in Algorithm 1) but still used sequential sampling. In the third experiment, we added sequential sampling to AC/LDA state-of-the-art ECG biometric features. The purpose of the first experiment is to present performance improvement of this paper's CA system over state-of-the-art works. The purpose of the second experiment is of three folds: first is to show that a system with 1DMRLBP with temporal variation extraction and sequential sampling outperforms 1DMRLBP with no temporal variation extraction but with sequential sampling. Also, to report and conclude that adding sequential sampling improves biometric results over the system with no sequential sampling in Section V-C; hence, sequential sampling purpose is not only for continuous authentication. The last purpose is to show that sequential sampling is applicable to 1DMRLBP that does not extract temporal variation. In implementing sequential sampling with AC/LDA in the third experiment, we desire to illustrate that sequential sampling application is not restricted to 1DMRLBP features and to reinforce that it adds biometrics improvement when compared to the same system but without sequential sampling.

Different parameters set up change the criterion of the sequential sampling. The results in Table III present performance with different parameters. These results were collected by training a model for each subject. Afterwards, the model was examined on all 1,012 database subjects, and FAR and FRR were collected. It can be noticed from Table III as how the FAR and FRR decrease as the sequential sampling criteria become more aggressive. It is more aggressive in a sense that the criteria are more difficult to meet. The more aggressive the criteria are the larger sample size that is required.

The choice of what parameters to use would be an application dependent. A heartbeat can be acquired at a rate of 1-1.5 heartbeat/second. If CA7 in Table III is considered, then around 30 observations are required to meet a criterion, which translates to around 24 seconds of ECG acquisition in comparison to 4 seconds in the case of CA1.

A state-of-the-art work of Ahmed and Traore [30] was one of the systems we adapted for ECG biometrics and was compared to the proposed CA system. In [30], proportion instead of *means* were used in the construction of the sequential sampling criteria. The equations for the criteria that separate the three regions are [30]:

$$\begin{aligned} UpperLine &= -h_1 + sl \times n \\ LowerLine &= h_2 + sl \times n \end{aligned} \tag{16}$$

where, $h_1 = \frac{1}{g}\left[log\left(\frac{1-\alpha}{\beta}\right)\right]$, $h_2 = \frac{1}{g}\left[log\left(\frac{1-\beta}{\alpha}\right)\right]$, $g = log\left[\frac{p_2(1-p_1)}{p_1(1-p_2)}\right]$, and $sl = \frac{1}{g}\left[log\left(\frac{1-p_1}{1-p_2}\right)\right]$. p_1 corresponds to the maximum probability to flag an imposter, and p_2 denotes the minimum probability before authenticating a genuine user. No hypothesis generation was needed, and the criteria were generated using different p_1 values while setting $p_2 = 1 - p_1$ [30]. Table IV presents the results. As it can be noticed from Table IV, changing p_1, α, and β influence the results. Ahmed and Traore [30] investigated these parameters choice in depth. However, the same concept of

TABLE IV
PERFORMANCE OF AHMED AND TRAORE [30] CA SYSTEM

#	p_1	$\alpha = \beta$	FRR	FAR	IO	GO
1	0.15	0.01	8.55%	9.30%	6.65	6.23
2	0.25	0.01	5.75%	8.82%	9.29	9.88
3	0.25	0.001	4.06%	7.33%	12.61	12.32
4	0.35	0.01	**4.33%**	**7.12%**	**14.22**	**14.19**
5	0.45	0.01	4.05%	10.33%	35.32	35.45

criteria aggressiveness explained in Section III-D regarding the width between the criteria lines applies to the work in [30].

By comparing Table III to Table IV, it can be noticed that on a fixed value of α and β, the proposed CA consistently achieved lower FRR and FAR, and it could reach a decision with less number of observations. Furthermore on a closely similar GO and IO values as in CA1 in Table III and #1 in Table IV, the proposed CA outperformed Ahmed and Traore [30]. Also, the minimum FAR and FRR reported in our proposed method was not achievable in Ahmed and Traore [30]. Hence, the proposed CA system performance surpasses a state-of-the-art from all examined aspects.

Another comparison to a state-of-the-art approach by Labati *et al.* [25] was conducted. The work in Labati *et al.* [25] applied different fusion techniques such as *mean*, *median*, 75^{th} percentile, 90^{th} percentile, 95^{th} percentile, and *max* on a predefined number of observations. A system with 1DMRLBP with n=1 as a feature extraction and bagging as a classier was used in the experiment. The main purpose of this experiment is to compare sequential sampling to fusion in implementing a CA system. Table V presents the results for different segment sizes.

In the work of Labati *et al.*, we do not have a dynamic number of GO and IO since a pre-determined number of observations is used. If we take 5 observations for example, then our approach achieved FRR of 1.13% and FAR of 8.11% (Table III) in comparison to an FRR of 3.93% and FAR of 9.69% (Table V) using Labati *et al. mean* fusion method. Similarly, other comparisons can be performed, and we can conclude that using sequential sampling outperforms the examined fusion methods.

Table III reveals that 1DMRLBP with temporal variation extraction consistently outperforms 1DMRLBP without temporal variation extraction. Therefore, the improvement achieved in considering 1DMRLBP in Section V-C propagates even after adding a sequential sampling. We can conclude that considering temporal variation enhances performance. Furthermore, if we compare 1DMRLBP with sequential sampling to same but without sequential sampling in both cases: considering temporal variation extraction and not considering temporal variation extraction, in other words compare Table III with Figure 8, the improvement of biometric performance after adding sequential sampling is apparent on both types of features.

Lastly, sequential sampling is not applicable to 1DMRLBP features only. Table VI presents the results when sequential sampling was applied to AC/LDA features. Adding sequential sampling also improved the performance of AC/LDA when compared to the AC/LDA without sequential sampling in Figure 9. On the other hand, comparing Table III versus Table VI, we can conclude that 1DMRLBP with sequential sampling outperforms AC/LDA with sequential sampling. For a fair comparison, one needs to compare the experiments where approximately same number of observations were used to make a decision. It can be noticed that 1DMRLBP with sequential sampling, whether we use n=1 or consider temporal variation extraction, outperforms that of AC/LDA. One important point to note while comparing the results is that CA2 and CA3 in Table III are to be compared to CA3 and CA4 in Table VI, respectively. The reason behind this is that AC/LDA is based on distance measure while 1DMRLBP is based on confidence measure. The smaller the distance the higher the similarity while the higher the confidence the higher the similarity to a class. As result, when we add a positive number to μ_1 (imposter mean) and subtract a positive number from μ_2 (genuine mean), we are making the means further apart in the AC/LDA experiment. Hence, the criteria become less aggressive. For this reason, CA4 in Table VI requires less number of IO and GO than CA1. This is identical to the scenario of adding a positive number to μ_2 (genuine mean) in 1DMRLBP and subtracting a positive number from μ_1 (imposter mean). Not all parameters in Table III could be applied to AC/LDA because doing so required a number of observations that exceeded the number of the database's subjects observations.

From these sequential sampling experiments, we conclude:

- Sequential sampling can be incorporated with 1DMRLBP and other features to achieve a CA system.
- Sequential sampling parameters control the aggressiveness of the CA system.
- Sequential sampling, apart from its advantage in achieving a CA system, enhances biometric performance.
- The more aggressive the system is, the higher the accuracy yet the higher IO and GO.
- The mechanism of feature extraction in Algorithm 1 is essential to sequential sampling algorithm since it results in only one feature vector from multiple observations; hence, no fusion or decision-making algorithms are needed.
- The proposed CA system outperforms state-of-the-art CA systems.

F. Continuous Authentication in Action

This experiment mimics CA operation in a real-life scenario. In real-life, CA continuously examines segments. Every segment ends by making a decision. To simulate a scenario, we constructed a lengthy stream of observations from different subjects, and we trained a subject. The subject's training and testing data did not overlap. The subject we trained was considered genuine while the others were considered imposters. Figure 10 simulates a CA system in action.

For this experiment, CA1 in Table III was used. When genuine observations were provided, authenticate criterion was reached while when imposters observations were encountered the reject criterion was met. Furthermore, in some segments, noise interfered and that required a bigger sample size to make

TABLE V
PERFORMANCE USING 1DMRLBP WITH N=1 USING CA METHODS IN LABATI *et al.* [25]

	Mean		Median		Max		75^{th} perc.		90^{th} perc.		95^{th} perc.	
Segment size	FAR%	FRR %	FAR %	FRR %	FAR %	FRR %	FAR %	FRR %	FAR %	FRR %	FAR %	FRR
5	9.69	3.93	10.84	5.95	34.12	0.50	21.19	1.11	34.12	0.50	34.12	0.50
10	8.71	2.36	9.3	2.56	44.63	0	21.39	0.20	36.32	0	44.63	0
15	8.15	2.06	9.12	2.61	50.11	0	19.74	0.55	35.94	0.13	45.25	0
20	7.81	0.77	8.40	1.35	54.78	0	19.94	0.19	35.86	0	47.24	0
30	7.38	1.00	7.98	1.50	60.53	0	20.04	0.25	35.59	0	47.36	0
40	7.08	0.35	7.66	0.70	63.14	0	218.91	0	34.71	0	46.10	0

TABLE VI
SEQUENTIAL SAMPLING PERFORMANCE AC/LDA [14]

	Parameters				AC/LDA [14] with sequential sampling			
CA number	H_1 mean	H_2 mean	α	β	FRR	FAR	IO	GO
CA1	μ_1	μ_2	0.01	0.01	5.88%	8.47%	18.11	17.13
CA2	$\mu_1 - 0.1\sigma$	$\mu_2 + 0.1\sigma$	0.01	0.01	6.95%	4.98%	25.43	19.17
CA3	$\mu_1 + 0.1\sigma$	$\mu_2 - 0.1\sigma$	0.01	0.01	6.59%	11.11%	14.17	14.61
CA4	$\mu_1 + 0.3\sigma$	$\mu_2 - 0.3\sigma$	0.01	0.01	5.44%	13.68%	9.76	11.16
CA5	μ_1	μ_2	0.001	0.001	6.67%	5.16%	24.79	19.58
CA6	μ_1	μ_2	0.0001	0.0001	10.76%	5.16%	30.28	20.08
CA7	μ_1	μ_2	0.01	0.001	9.46%	5.65%	24.78	17.14
CA8	μ_1	μ_2	0.001	0.01	4.11%	11.80%	18.15	19.58
CA9	μ_1	μ_2	0.1	0.01	9.65%	6.36%	17.91	11.36
CA10	μ_1	μ_2	0.01	0.10	3.37%	21.76%	9.97	16.97

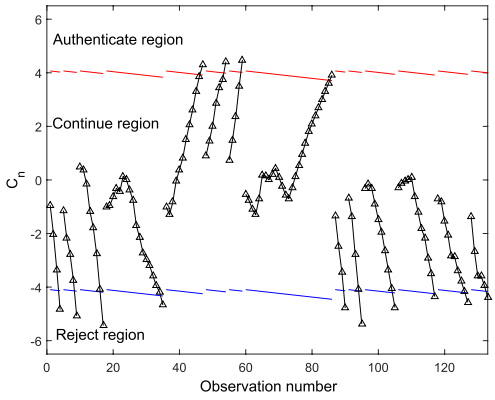

Fig. 10. A simulated CA performance. Each triangle corresponds to an observation, and its value is C_n. The line that connects a set of triangles represents the segment that was used to reach a decision. The upper and the lower lines illustrate the decision threshold variations for that segment.

a decision. This is obvious from segment 4 and segment 8 in Figure 10. Also, these two segments lie at the boundaries where imposter and genuine observations were mixed within one segment, which is a possible real-life scenario.

We can conclude from this experiment that this CA system can tolerate noise and can change sample size and decision thresholds during run-time based on previous observations confidences.

VI. CONCLUSION

A continuous authentication system that is capable of monitoring subjects continuously and flag intruders was presented. This system dynamically decides on the number of observations needed and adaptively sets the acceptance/rejection threshold to make a decision. Such capability was achieved by proposing One Dimensional Multi-Resolution Local Binary Patterns (1DMRLBP) features and utilizing sequential sampling. 1DMRLBP extracts ECG heartbeats temporal variation from several observations and constructs one feature vector from them. Without this property, continuous authentication system needs a fusion stage. Sequential sampling is a statistical method that has two criteria on which the result would be either to verify identity, reject identity, or request more observations. Because of sequential sampling, decision thresholds are not pre-set and are updated based on the number of observations examined.

1DMRLBP was examined on two databases: PTB, for medical applications; and UofTDB, for biometrics application. The biometric system achieved EER of 7.89% on UofTDB 1,012 single session subjects in comparison to 12.30% from a state-of-the-art approach. It also resulted an EER of 10.10% in UofTDB 82 multiple sessions subjects. The continuous authentication system successfully reported an FRR of 0.39% and FAR of 1.57% with an average segment size of around 32 observations. If small number of observations is desired, then it achieved 1.93% FRR and 9.68% FAR with an average segment size of around 4 observations. The proposed continuous authentication system showed superiority in performance over the examined state-of-the-art works. With their properties, 1DMRLBP and sequential sampling each by itself or together as a CA system can be deployed for other applications.

APPENDIX
REVIEW OF TEMPORAL AND SPATIAL LOCAL BINARY PATTERNS

Several 2D LBP variants attempted extracting temporal and spatial variation from observations. While they achieved promising results in their designated applications, they are not suitable for the application proposed in this paper. In [43], the authors proposed Volume Local Binary Patterns (VLBP).

VLBP feature type extracts LBP features for pixels from three frames, and it gives different weight to each of the three frames. From these frames, VLBP extracts features from co-occurred pixels on three orthogonal planes. The resultant histogram would be of a length of 3.2^p bins, where p is the number of points to consider around a desired pixel. VLBP was proposed for offline applications (i.e. the entire experimented database should be available beforehand). In comparison to 1DMRLBP, 1DMRLBP extracts features with any number of observations. It also constructs a constant number of bins regardless of the number of observations it is extracted from. Lastly, 1DMRLBP can be used for online applications.

In [52], the authors acknowledged the long feature vector of [43] and proposed a fix to that issue. They introduced two techniques to reduce the number of bins, yet the issues of being an offline approach and an approach that considers only three frames persisted. First technique proposed to use 6 unique points from the three orthogonal planes. The second method dealt with reducing the number of features by taking the average value of orthogonal planes points.

The work in [44] proposed Spatio-Temporal Local Binary Patterns (STLBP). This type of features is online and applicable for real-time applications. For each pixel, it extracts the binary patterns for that observation using its current neighbors, then it extracts binary patterns from the same pixel location but from different observations. The feature vector is compiled of two histograms: one from the current observation and the other is from the previous observation. Unlike [44], 1DMRLBP has a smaller feature vector, models temporal progression over any number of observations, and lastly, it holistically considers progression of distribution of whole observation rather than for single pixels. The work in [53] extracts spatial and temporal LBP by prediction. It uses previous frames to predict the value of a pixel in the current frame. It compares the predicted value against the actual value and incorporates that value in the LBP feature extraction method.

ACKNOWLEDGMENT

The authors would like to thank Shahad Abdulnour for her input and expertise.

REFERENCES

[1] W. Louis, D. Hatzinakos, and A. Venetsanopoulos, "One dimensional multi-resolution local binary patterns features (1DMRLBP) for regular electrocardiogram (ECG) waveform detection," in *Proc. 19th Int. Conf. Digit. Signal Process.*, Aug. 2014, pp. 601–606.

[2] W. Louis and D. Hatzinakos, "Enhanced binary patterns for electrocardiogram (ECG) biometrics," in *Proc. Can. Conf. Elect. Comput. Eng.*, 2016.

[3] I. Traore and A. A. E. Ahmed, *Continuous Authentication Using Biometrics: Data, Models, and Metrics*. Information Science Reference, 2012.

[4] C. M. Carrillo, "Continuous biometric authentication for authorized aircraft personnel: A proposed design," M.S. thesis, Naval Postgraduate School, Monterey, CA, USA, 2013.

[5] B. Toth, "Biometric liveness detection," *Inf. Security Bull.*, vol. 10, no. 8, pp. 291–297, 2005.

[6] M. Suresh, P. G. Krishnamohan, and M. S. Holi, "Electromyography analysis for person identification," *Int. J. Biometrics Bioinformat.*, vol. 5, no. 3, pp. 172–179, 2011.

[7] I. Odinaka, P.-H. Lai, A. Kaplan, J. A. O'Sullivan, E. J. Sirevaag, and J. W. Rohrbaugh, "ECG biometric recognition: A comparative analysis," *IEEE Trans. Inf. Forensics Security*, vol. 7, no. 6, pp. 1812–1824, Dec. 2012.

[8] J. F. Hu and Z. D. Mu, "Authentication system for biometric applications using mobile devices," *Appl. Mech. Mater.*, vols. 457–458, pp. 1224–1227, Oct. 2014.

[9] G. D. Clifford, F. Azuaje, and P. McSharry, *Advanced Methods and Tools for ECG Data Analysis*. London, U.K.: Artech House, 2006.

[10] M. S. Thaler, *The Only EKG Book You'll Ever Need*, vol. 365, 2nd ed. Norwell, MA, USA: Kluwer, 2007.

[11] T. Ojala, M. Pietikäinen, and T. Mäenpää, "Multiresolution gray-scale and rotation invariant texture classification with local binary patterns," *IEEE Trans. Pattern Anal. Mach. Intell.*, vol. 24, no. 7, pp. 971–987, Jul. 2002.

[12] G. E. Forsen, M. R. Nelson, and R. J. Staron, Jr., *Personal Attributes Authentication Techniques*. Rome, NY, USA: Pattern Analysis and Recognition Corp., 1977.

[13] L. Biel, O. Pettersson, L. Philipson, and P. Wide, "ECG analysis: A new approach in human identification," *IEEE Trans. Instrum. Meas.*, vol. 50, no. 3, pp. 808–812, Jun. 2001.

[14] F. Agrafioti, "ECG in biometric recognition: Time dependency and application challenges," Ph.D. dissertation, Dept. Electr. Comput. Eng., Univ. Toronto, Toronto, ON, Canada, 2011.

[15] F. Agrafioti and D. Hatzinakos, "Fusion of ECG sources for human identification," in *Proc. IEEE Int. Symp. Commun., Control Signal Process.*, Mar. 2008, pp. 1542–1547.

[16] K. N. Plataniotis, D. Hatzinakos, and J. K. M. Lee, "ECG biometric recognition without fiducial detection," in *Proc. IEEE Biometrics Symp., Special Session Res. Biometric Consortium Conf.*, Sep./Aug. 2006, pp. 1–6.

[17] J. M. Irvine and S. A. Israel, "A sequential procedure for individual identity verification using ECG," *EURASIP J. Adv. Signal Process.*, vol. 2009, pp. 1–13, May 2009.

[18] S. Z. Fatemian and D. Hatzinakos, "A new ECG feature extractor for biometric recognition," in *Proc. IEEE Int. Conf. Digit. Signal Process.*, Jul. 2009, pp. 1–6.

[19] C.-C. Chiu, C.-M. Chuang, and C.-Y. Hsu, "A novel personal identity verification approach using a discrete wavelet transform of the ECG signal," in *Proc. IEEE Int. Conf. Multimedia Ubiquitous Eng.*, Apr. 2008, pp. 201–206.

[20] M. Li and S. Narayanan, "Robust ECG biometrics by fusing temporal and cepstral information," in *Proc. IEEE Int. Conf. Pattern Recognit. (ICPR)*, Aug. 2010, pp. 1326–1329.

[21] C.-K. Chen, C.-L. Lin, S.-L. Lin, Y.-M. Chiu, and C.-T. Chiang, "A chaotic theoretical approach to ECG-based identity recognition [application notes]," *IEEE Comput. Intell. Mag.*, vol. 9, no. 1, pp. 53–63, Feb. 2014.

[22] A. D. C. Chan, M. M. Hamdy, A. Badre, and V. Badee, "Wavelet distance measure for person identification using electrocardiograms," *IEEE Trans. Instrum. Meas.*, vol. 57, no. 2, pp. 248–253, Feb. 2008.

[23] F. Agrafioti and D. Hatzinakos, "ECG based recognition using second order statistics," in *Proc. IEEE 6th Annu. Commun. Netw. Services Res. Conf.*, May 2008, pp. 82–87.

[24] Z. Zhao, L. Yang, D. Chen, and Y. Luo, "A human ECG identification system based on ensemble empirical mode decomposition," *Sensors*, vol. 13, no. 5, pp. 6832–6864, 2013.

[25] R. D. Labati, R. Sassi, and F. Scotti, "ECG biometric recognition: Permanence analysis of QRS signals for 24 hours continuous authentication," in *Proc. IEEE Int. Workshop Inf. Forensics Secur. (WIFS)*, Nov. 2013, pp. 31–36.

[26] M. Guennoun, N. Abbad, J. Talom, S. M. M. Rahman, and K. El-Khatib, "Continuous authentication by electrocardiogram data," in *Proc. IEEE Int. Conf. Sci. Technol. Humanity (TIC-STH)*, Sep. 2009, pp. 40–42.

[27] D. P. Coutinho, A. L. Fred, and M. A. Figueiredo, "ECG-based continuous authentication system using adaptive string matching," in *Proc. Biosignals*, 2011, pp. 354–359.

[28] D. P. Coutinho, A. L. Fred, and M. A. Figueiredo, "One-lead ECG-based personal identification using Ziv–Merhav cross parsing," in *Proc. IEEE Int. Conf. Pattern Recognit. (ICPR)*, Aug. 2010, pp. 3858–3861.

[29] S. Mondal and P. Bours, "A computational approach to the continuous authentication biometric system," *Inf. Sci.*, vol. 304, pp. 28–53, May 2015.

[30] A. A. E. Ahmed and I. Traore, "Dynamic sample size detection in continuous authentication using sequential sampling," in *Proc. ACM 27th Annu. Comput. Secur. Appl. Conf.*, 2011, pp. 169–176.

[31] C. Shen, Z. Cai, and X. Guan, "Continuous authentication for mouse dynamics: A pattern-growth approach," in *Proc. IEEE Int. Conf. Dependable Syst. Netw. (DSN)*, Jun. 2012, pp. 1–12.

[32] D. El Menshawy, H. M. O. Mokhtar, and O. Hegazy, "A keystroke dynamics based approach for continuous authentication," in *Proc. 10th Int. Conf. Beyond Databases, Archit., Struct. (BDAS)*, 2014, pp. 415–424.

[33] P. Bours and S. Mondal, "Continuous authentication with keystroke dynamics," in *Recent Advances in User Authentication Using Keystroke Dynamics Biometrics*, vol. 2, Y. Zhong and Y. Deng, Eds. Burlington, MA, USA: Science Gate Publishing, 2015, ch. 3.

[34] L. Breiman, "Bagging predictors," *Mach. Learn.*, vol. 24, no. 2, pp. 123–140, 1996.

[35] Y. Wang, F. Agrafioti, D. Hatzinakos, and K. N. Plataniotis, "Analysis of human electrocardiogram for biometric recognition," *EURASIP J. Adv. Signal Process.*, vol. 2008, pp. 1–11, Dec. 2008.

[36] J. Pan and W. J. Tompkins, "A real-time QRS detection algorithm," *IEEE Trans. Biomed. Eng.*, vol. BME-32, no. 3, pp. 230–236, Mar. 1985.

[37] I. Odinaka *et al.*, "ECG biometrics: A robust short-time frequency analysis," in *Proc. IEEE Int. Workshop Inf. Forensics Secur. (WIFS)*, Dec. 2010, pp. 1–6.

[38] J. Yao and Y. Wan, "Improving computing efficiency of a wavelet method using ECG as a biometric modality," *Int. J. Comput. Netw. Secur.*, vol. 2, no. 1, pp. 15–20, 2010.

[39] D. Jang, S. Wendelken, and J. M. Irvine, "Robust human identification using ECG: Eigenpulse revisited," *Proc. SPIE*, vol. 7667, p. 76670M, Apr. 2010.

[40] N. Chatlani and J. J. Soraghan, "Local binary patterns for 1-D signal processing," in *Proc. Eur. Signal Process. Conf. (EUSIPCO)*, 2010, pp. 95–99.

[41] Q. Zhu, N. Chatlani, and J. J. Soraghan, "1-D Local binary patterns based VAD used INHMM-based improved speech recognition," in *Proc. IEEE Eur. Signal Process. Conf. (EUSIPCO)*, Aug. 2012, pp. 1633–1637.

[42] L. Houam, A. Hafiane, A. Boukrouche, E. Lespessailles, and R. Jennane, "One dimensional local binary pattern for bone texture characterization," *Pattern Anal. Appl.*, vol. 17, no. 1, pp. 179–193, 2014.

[43] G. Zhao and M. Pietikäinen, "Dynamic texture recognition using local binary patterns with an application to facial expressions," *IEEE Trans. Pattern Anal. Mach. Intell.*, vol. 29, no. 6, pp. 915–928, Jun. 2007.

[44] S. Zhang, H. Yao, and S. Liu, "Dynamic background modeling and subtraction using spatio-temporal local binary patterns," in *Proc. 15th IEEE Int. Conf. Image Process. (ICIP)*, Oct. 2008, pp. 1556–1559.

[45] W. Louis and K. N. Plataniotis, "Co-occurrence of local binary patterns features for frontal face detection in surveillance applications," *EURASIP J. Image Video Process.*, vol. 2011, no. 1, p. 745487, 2011.

[46] C. Cortes and V. Vapnik, "Support-vector networks," *Mach. Learn.*, vol. 20, no. 3, pp. 273–297, 1995.

[47] A. Wald, "Sequential tests of statistical hypotheses," *Ann. Math. Statist.*, vol. 16, no. 2, pp. 117–186, 1945.

[48] C. J. Krebs, *Ecological Methodology*, 3rd ed. 2014. [Online]. Available: http://www.zoology.ubc.ca/~krebs/books.html

[49] S. Pouryayevali, S. Wahabi, S. Hari, and D. Hatzinakos, "On establishing evaluation standards for ECG biometrics," in *Proc. IEEE Int. Conf. Acoust., Speech Signal Process. (ICASSP)*, May 2014, pp. 3774–3778.

[50] R. D. De Veaux, P. F. Velleman, D. E. Bock, A. M. Vukov, and A. Wong, *Stats: Data and Models, First Canadian Edition*. Boston, MA, USA: Addison-Wesley, 2012.

[51] A. L. Goldberger *et al.*, "Physiobank, physiotoolkit, and physionet: Components of a new research resource for complex physiologic signals," *Circulation*, vol. 101, no. 23, pp. e215–e220, 2000.

[52] Y. Wang, J. See, R. C.-W. Phan, and Y.-H. Oh, "Efficient spatio-temporal local binary patterns for spontaneous facial micro-expression recognition," *PLoS ONE*, vol. 10, no. 5, p. e0124674, 2015.

[53] A. Shimada and R.-I. Taniguchi, "Hybrid background model using spatial-temporal LBP," in *Proc. 6th IEEE Int. Conf. Adv. Video Signal Based Surveill. (AVSS)*, Sep. 2009, pp. 19–24.

Wael Louis (S'07) received the B.Eng. degree (Hons.) in electrical engineering from Ryerson University, Canada, in 2008, and the M.A.Sc. degree from The Edward S. Rogers Sr. Department of Electrical and Computer Engineering, University of Toronto, Canada, in 2010. He is currently pursuing the Ph.D. degree with the Communication Group, Electrical and Computer Engineering Department, University of Toronto. His research interests lie in the areas of computer vision, signal and image processing, and biometric systems. He is a recipient (twice) of the Alexander Graham Bell Canada Graduate Scholarship for both M.A.Sc. and Ph.D. levels. He has also received the Ontario Graduate Scholarship.

Majid Komeili (S'08) received the M.Sc. degree in electrical engineering from Tarbiat Modares University, Tehran, Iran, in 2008. He is currently pursuing the Ph.D. degree in electrical engineering with the University of Toronto, Toronto, ON, Canada. Since 2012, he has been a Research Assistant and a Teaching Assistant with the Edward S. Rogers Sr. Department of Electrical and Computer Engineering, University of Toronto, Toronto, ON, Canada. His research interests include signal, image, and video processing, specifically ECG and EEG signal analysis, machine learning, machine vision, video surveillance, and document image processing.

Dimitrios Hatzinakos (F'16) received the Diploma degree from the University of Thessaloniki, Greece, in 1983, the M.A.Sc. degree from the University of Ottawa, Canada, in 1986, and the Ph.D. degree from Northeastern University, Boston, MA, USA, in 1990, all in electrical engineering. In 1990, he joined the Department of Electrical and Computer Engineering, University of Toronto, where he holds the rank of Professor with tenure. He served as the Chair of the Communications Group of the Department from July 1999 to June 2004. From 2004 to 2014, he was the Bell Canada Chair in Multimedia with the University of Toronto. Since 2007, he has been the Director and the Chair of the Management Committee of the Identity, Privacy and Security Institute with the University of Toronto. His research interests are in the areas of multimedia signal processing, multimedia security, multimedia communications and biometric systems.

He has authored or coauthored over 300 papers in technical journals and conference proceedings and he has contributed to 17 books in his areas of interest. His experience includes consulting through Electrical Engineering Consociates Ltd. and contracts with United Signals and Systems Inc., Burns and Fry Ltd., Pipetronix Ltd., Defense Research and Development Canada, Nortel Networks, Vivosonic Inc., CANAMET Inc., and OLG. He was an Associate Editor of the IEEE TRANSACTIONS ON MOBILE COMPUTING from 2011 to 2014. He served as an Associate Editor of the IEEE TRANSACTIONS ON SIGNAL PROCESSING from 1998 to 2002 and a Guest Editor of the special issue of *Signal Processing* (Elsevier) on Signal Processing Technologies for Short Burst Wireless Communications which appeared in October 2000. He was a member of the IEEE Statistical Signal and Array Processing Technical Committee from 1992 to 1995 and the Technical Program Co-Chair of the 5th Workshop on Higher-Order Statistics in 1997. He is a Fellow of the Canadian Institute of Engineering and a member of the Professional Engineers of Ontario and the Technical Chamber of Greece.